Thermophysics and Aeromechanics, *2019*, *Vol. 26*, *No. 1*

DOI: 10.1134/S0869864319010086

Experimental investigation of structure and heat transfer in cellular flame of rich and lean propane-butane-air mixtures[*]

B.F. Boyarshinov, S.Yu. Fedorov, and R.Kh. Abdrakhmanov

Kutateladze Institute of Thermophysics SB RAS, *Novosibirsk*, *Russia*

E-mail: boyar@itp.nsc.ru

(*Received July 09*, *2018*; *revised September 07*, *2018*; *accepted for publication October 11*, *2018*)

We studied a lean propane-butane-air mixture ascending through a round hole of 10-mm diameter, covered by a brass mesh as a single element of the multicellular flame. Gas temperature was measured by the CARS method (Coherent anti-Stokes Raman Scattering) with original software for spectra processing. The vertical and horizontal velocity components were measured by the PIV method (Particle Image Velocimetry). Distributions of heat release intensity and heat fluxes, which cannot be obtained in direct measurements, were estimated using balance relationships in the energy equation. The results were compared with the data obtained for the rich mixture flame in experiments with the same burner. Convective and molecular heat fluxes were considered separately. It was shown that when the rich air mixture with propane-butane burns, the heat flux caused by thermal conductivity reach a maximum at the center of the heat-release zone. Their intensity is substantially lower in comparison with the convective fluxes behind the flame front, which in turn are almost twice as weak as the convective flux in the flame of a lean mixture. The maximal intensities of heat release in the flame of a rich mixture are lower than in the lean one.

Key words: cellular flame, Particle Image Velocimetry (PIV), Coherent anti-Stokes Raman Scattering (CARS), balance method.

Introduction

Regularities related to heat fluxes at gas motion without chemical interaction with the channel walls are widely represented in various publications levels. Experimental studies are known [1], where the data on heat fluxes are obtained not only on the wall, but also near it.

Heat generation and its transfer are the most important features of the combustion process. To describe heat transfer it is important to know the value and distribution of heat fluxes in every specific case. As a result of solving the integral relations for the reacting boundary layer as well as in the course of numerical simulation, distribution of thermal parameters in a chemically reacting boundary layer was obtained. Reviews of publications dealing with the study of this process can be found in [2, 3].

In numerous experimental studies in the flows with combustion, heat transfer is considered at chemical reaction of substances in various aggregative states. Heat transfer of solids such as

---

[*] The work was financially supported by FASO and RFBR (Project No. 18-03-00282).

polymethyl methacrylate was studied in [4–6], burnout of the walls of a graphite channel was described in the monograph [7], evaporation and combustion of liquid fuel were considered in [8–10], injection of gaseous fuel, including hydrogen, was studied in [11–13]. These studies are usually associated with obtaining data on heat fluxes on the channel walls, confining the flow of a chemically reacting gas. In this case, the value of heat fluxes is estimated either from the temperature profiles [6] or by the measurements of substance fluxes on the wall [7–10]. In experiments on ethanol combustion with the formation of a cellular flame front [14, 15], it was shown that three-dimensional large-scale cellular structures increase significantly (up to three times) the intensity of mass transfer on the channel wall as compared to substance transfer in a chemically reacting laminar boundary layer. In these works, there are no data on distribution of heat fluxes at combustion in the volume of a moving gas. The authors do not know the experimental studies, where data on energy fluxes far from the walls, including the vicinity of the cellular flame front, would be obtained. Such information is useful when analyzing stability of combustion and solving the problems of flame propagation and flameout.

For the gas flow with chemical transformations, heat release is the most important parameter and the origin of transfer processes. It was noted in [16] that the problem of determining the rate of heat generation is complicated by the necessity to know the components of the mixture, occurring chemical reactions (direct and reverse), and their rate. The amount of empirical information on heat release is limited. In [17], the intensity of heat release during chemical reaction was investigated. It was shown that it varies widely depending on organization of the combustion process: from 0.01 to 6 GW/m^3. Under laboratory conditions, the heat release rate was approximately 350–400 MW/m^3 [18], and its estimated value in fires was 1.1 MW/m^3 [19].

The temperature gradients, initiating heat transfer, are formed during heat generation. The characteristic size of the heat-release region (the half-width of the temperature gradient profile at its half-height) is ~ 0.5 mm according to the data of [20]. In experiments of [21], the half-width of the temperature profile was up to 2 mm. Thus, the known diagnostic methods with spatial resolution of about 0.1 mm can be used for the experimental study of heat transfer processes. For empirical data processing, it is possible to use the transport equations, including temperature gradients, velocities, and thermophysical parameters presented as a grid with a step of ~ 0.1 mm.

The purpose of this work is to obtain the data on distribution of heat release and heat fluxes in a vicinity of the front of chemical reaction relative to the cellular flame of propane-butane-air mixture.

1. Object of research and equipment

The object of research is a cellular flame formed at combustion of the propane-butane-air mixture in an ascending flow (Fig. 1). In the general case, the flame is non-stationary, and the moving cells in it are easily displaced and deformed when the probes are introduced into the combustion zone. In [22], it was shown that with a decrease in the initial jet diameter, a single stationary cell can be distinguished, whose characteristics are similar to the elements of multicellular flame. In our study, a burner with an outlet diameter of 10 mm was used. A mesh of brass wire with the 0.15-mm diameter and cell size of 0.3×0.3 mm was soldered to the edges of the hole. In front of the cavity outlet with the diameter of 27 mm, there were three layers of the same mesh. The equivalent ratio in the rich mixture was Φ = 1.4–1.6. With a further decrease in the share of propane-butane to Φ = 0.9, the flame front turned to another stationary shape. By the analogy with rotating chemically reacting jets [23], these two shapes of flame, on the basis of appearance, are conventionally called M-flame (for a rich mixture) and V-flame (for a lean mixture). In experiments on heat transfer, domestic liquefied gas from a balloon was used. Composition of the combustion products and composition of the initial mixture were not measured. Equivalent ratio Φ in the usual form [24] was estimated as

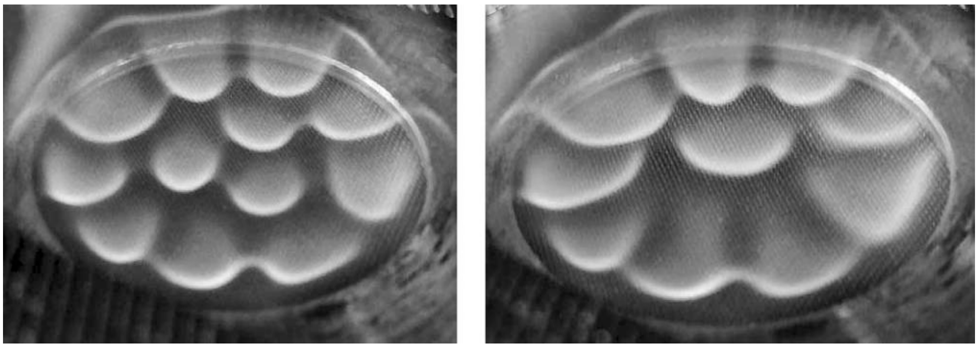

Fig. 1. Cellular flame in the ascending flow of rich propane-butane-air mixture (equivalent ratio $\Phi = 1.4$) above the hole of 24-mm diameter, covered by a brass mesh. Variability of the flame shape and known visual effect of "a drop on the ceiling".

the ratio of the volume flow rate of combustible gas and air to the corresponding stoichiometric ratio under the assumption that propane is the main component of the fuel.

The local characteristics of stationary two-dimensional V-flame of lean propane-butane-air mixture ($\Phi = 0.9$, Re = 543, the ratio of propane-butane and air flow rates (ml/s) was 4/110) were studied to understand the effect of combustible mixture dilution on the structure and heat transfer in a cellular flame. In [25, 26], propagation of a similar (tulip-like) flame inside a channel was studied. The detached V-flame of an ascending jet in the open air can be considered as a type of tulip-like flame front. It can be seen in Fig. 2 that in contrast to the shape of the rich mixture flame, a lean mixture flame does not form a conical surface above the flame front. When analyzing the experiments (see Fig. 3), we used the primary data obtained for the M-flame of rich mixture on the same burner ($\Phi = 1.4$, Re = 370, the ratio of propane-butane and air flow rates (ml/s) was 4/75).

To obtain experimental data on the velocity and temperature fields in a lean flame, we used the same optical equipment as in experiments with a rich mixture [22]. The gas flow with submicron particles was twice illuminated with laser light, and two consecutive images were taken. The time period between pulses was 23 ms. The local flow velocity was calculated by a change in the position of particles in these images by applying the cross-correlation algorithm. Data were collected and processed by a PC with ActualFlow software. Without combustion, velocity measurements at the hole outlet (at distance $y \sim 1$ mm from the mesh and at a distance from the jet axis $r < 4$ mm) showed that the flow is uniform over the radius with accuracy $\Delta V/V \approx 10$ %. The profiles of longitudinal velocity of gas moving away from the wall are presented in Fig. 4. It is seen that as the flame front approaches (marked by the symbols), velocity component V somewhat decreases, and at a distance of ~ 8 mm, it reaches the highest values. The gas velocity increases with increasing radial coordinate of the glowing flame surface.

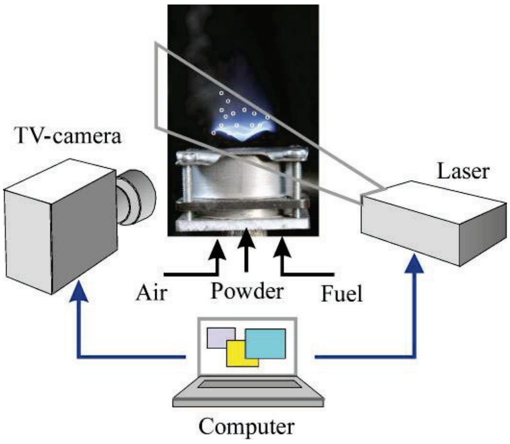

Fig. 2. Flame of lean mixture (V-flame). PIV scheme for measuring 2D field of gas velocity.

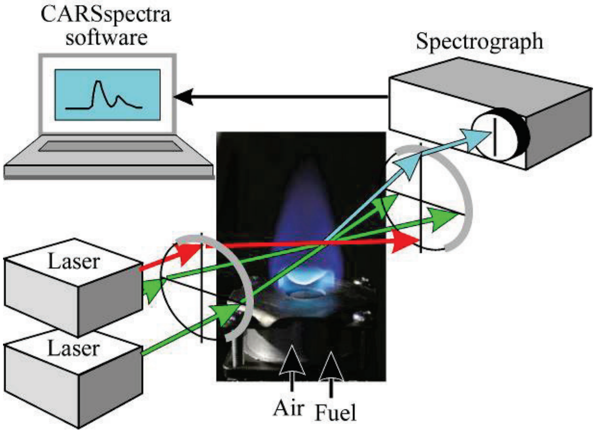

Fig. 3. Flame of rich mixture (M-flame).
Scheme of the CARS method for measuring
the local temperatures.

To measure the gas temperature, the CARS (Coherent Anti Stokes Scattering) method, based on registration of radiation excited in the intersection region of laser beams with specified properties, was used. To measure the temperature, we recorded the spectra of nitrogen in the initial mixture, in the flame front, and in the combustion products. Two beams in Fig. 3 (light gray arrows) with wavelength of λ = 532 nm and energies of 12 mJ/imp and a beam of broadband radiation with λ = 607 nm (black arrow) of the tunable laser were focused and intersected according to the “boxcars” scheme. A measuring volume of 0.1×0.1×1 mm was formed at the intersection. The CARS beam in the measuring volume, spatially separated from the laser beams, was focused on the inlet slit of the DFS-24 double monochromator with a multichannel optical spectra recorder. The temperature was calculated according to the shape of the spectrum using the CARSspectra software [27].

In Fig. 5, the triangular symbols show the results of CARS measurements of the V-flame temperature for two extreme values of the radius of the burning lean mixture, when r = 0 mm and r = 6 mm. Intermediate values are represented by the profiles, used then in the balance method. The calculation results were smoothed by the B-spline. It can be seen that, in fact, the glowing flame front (its position is marked with the square symbols) in the lean mixture is an isothermal surface $T \sim 1100 \pm 50$ K. The temperature gradients are important, when processing experimental data with the use of the transport equations. The value of gradients (~ 1700 K/mm for r = 6 mm in Fig. 5) was close to experimental data of [21], where it was ~ 1800 K/mm (diffusion combustion of a methane counter-jet, which was studied by the method of spontaneous Raman scattering).

According to comparison of data presented in Figs. 4 and 5, the rate of temperature increase from the initial to the final value exceeds significantly the rate of an increase in the gas velocity. Gas heating is faster than its expansion, and this can be a reason for a local increase in the static pressure behind the lean flame front. The presence of local areas of

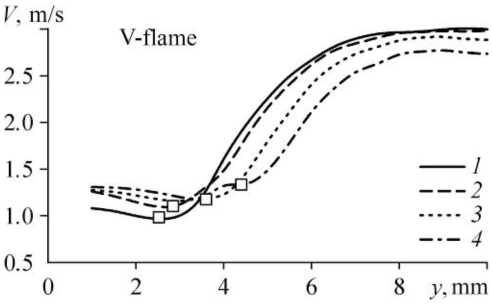

Fig. 4. Field of longitudinal velocity component at combustion of lean propane-butane-air mixture.
Symbols indicate the position of the flame contour; lines — profiles for r = 0 (*1*), 1 (*2*), 2 (*3*), 3 mm (*4*).

Fig. 5. Temperature profiles in the flame of lean propane-butane-air mixture.

Square symbols indicate the position of the visible flame contour, triangles — results of CARS-measurements for $r = 0$ mm and $r = 6$ mm; lines — profiles for $r = 0$ mm (*1*), 1 mm (*2*), 2 mm (*3*), 3 mm (*4*), 4 mm (*5*), 5 mm (*6*), 6 mm (*7*).

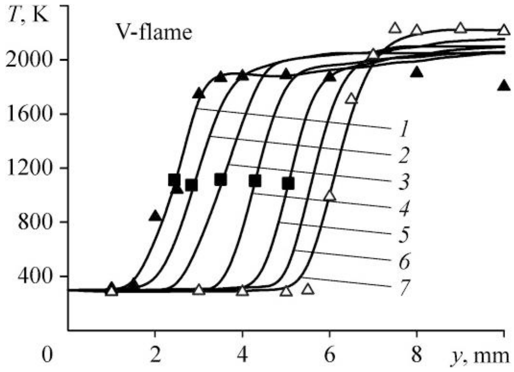

increased static pressure near the front of the cellular flame was noted in [28]. The value of this parameter by the estimates of [22] is approximately 0.5 Pa.

2. The objective of research and method of processing the measurement results

The main objective of the study was to assess the intensity of heat transfer in the vicinity of laminar flames of type M and V. By their characteristics, they are close to the multicellular flames of the ascending jets of rich and lean propane-butane-air mixtures, and this makes it possible to determine the effect of the degree of combustible gas dilution on heat flux distribution. The intensity of heat fluxes was calculated by the experimental data on local temperature and velocity profiles. In the course of research, the parameters of gas at combustion of lean and rich mixtures were compared and correlated with the position of characteristic regions in the vicinity of the combustion zone, where the heat release maximum is formed and where the glow visualizes the flame surface.

To process the obtained experimental data, we applied the balance method, which was used to estimate turbulent stresses [9], rates of substance formation [29], and rates of heat release [22]. In this method, the measurement results are presented in the form of a two-dimensional grid of the local gas parameters depending on the radial coordinate and distance from the burner cut with a step of 0.125 mm so that two velocity components and temperature would be known at each grid point. The local values of heat capacity, viscosity, and heat conductivity were additionally determined from the temperature. Further, the finite differences of parameters at the grid nodes were used in the transport equations instead of their derivatives. After each differentiation procedure, the calculation results were smoothed by the B-spline.

The possibility of obtaining the data on heat fluxes in the gas volume far from the wall was checked when processing the experiments in which turbulent heat fluxes were measured in a two-dimensional boundary layer without burning. The authors of [1] determined the heat fluxes by measuring fluctuations of temperature T' and velocity U', i.e., from expression $q^{\mathrm{T}} = \rho C_{\mathrm{P}} \overline{U'T'}$. In the same paper, data on distributions of average values of temperature T and velocity components U and V were presented. We use the above method to find the same turbulent heat fluxes using the balance method, i.e., substituting averaged values $T(x, y)$, $U(x, y)$, and $V(x, y)$ into the energy equation with subsequent integration:

$$q^{\mathrm{T}} = \int_0^y \left(C_{\mathrm{P}} \rho U \frac{\partial T}{\partial x} + C_{\mathrm{P}} \rho V \frac{\partial T}{\partial y} - \frac{\partial}{\partial y}\left(\lambda \frac{\partial T}{\partial y} \right) - U \frac{\partial P}{\partial x} \right) \partial y. \qquad (1)$$

Experiments of [1] were carried out in an air flow, whose velocity increased along the length of the channel. Results of integration (1) and results of direct measurements of the turbulent heat fluxes by velocity and temperature pulsations are compared in Fig. 6. The line shows integration results for acceleration parameter $Kr = (x / U_0) \cdot (dU_0 / dx) = 0.15 \cdot 10^{-3}$

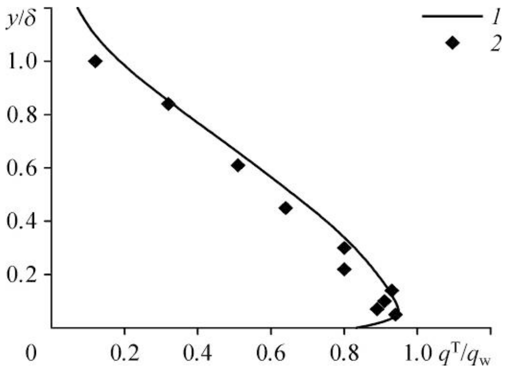

Fig. 6. Comparison of results of determining the turbulent heat flux by the balance method (*1*) and direct measurements [1] (*2*).

during processing of the experiment denoted as 040175. The symbols correspond to q^T data determined from the joint measurements of temperature and velocity fluctuations. The abscissa axis represents the value of the turbulent heat flux ratio to the wall flow q^T / q_w, which was determined based on the data on Stanton number $q_w = \text{St} \times \rho_0 U_0 \cdot C_P \cdot (T_w - T_0)$ for longitudinal coordinate x = 1473 mm and boundary layer thickness δ = 26 mm. The figure shows that the balance method can be applied for determining the heat fluxes in the volume of moving gas without chemical transformations.

To process experimental data in an axisymmetric flow with combustion, in the first approximation, it is proposed to use the energy equation, where Lewis–Semenov number is Le = 1:

$$\left(\frac{\partial(\rho C_P T \cdot V)}{\partial y} + \frac{1}{r} \cdot \frac{\partial(\rho C_P T \cdot U)}{\partial r}\right) = \frac{\partial}{\partial y}\left(\lambda \frac{\partial T}{\partial y}\right) + \frac{1}{r} \cdot \frac{\partial}{\partial r}\left(r \cdot \lambda \frac{\partial T}{\partial r}\right) + W, \tag{2}$$

here, V and U (m/s) are components of the velocity vector in direction y (m), i.e., upward the jet axis and along its radius r (m); T (K) is the local temperature of the gas mixture as a function of coordinates $T(x, y)$ in the flame, W (W/m^3) is heat release rate, C_P (J/kg/K) is heat capacity, ρ (kg/m^3) is density, λ (W/m/K) is heat conductivity, μ (kg/s/m) is the dynamic viscosity. Dependence of thermophysical parameters (C_P, λ, μ) on temperature was taken the same as that for nitrogen.

For the used PIV equipment, the accuracy of data on longitudinal velocity component V was ~ 5 % and it was higher than the accuracy of determining horizontal component U. Therefore, in this work, instead of experimental data, we used the values of U calculated from the measurements of longitudinal component V by the continuity equation in cylindrical coordinates:

$$\frac{\partial(r\rho V)}{\partial y} = -\frac{\partial(r\rho U)}{\partial r}. \tag{3}$$

Density ρ was calculated by the temperature from the equation of state taking into account that in experiments, the molecular weight of the mixture changes insignificantly: $\rho = \rho_0 \cdot (T_0 / T)$, ρ_0 = 1.21 kg/m^3, T_0 = 298 K.

When integrating, differentials were replaced by finite differences (the step in both coordinates was 0.125 mm). Measurements of the radial velocity, performed using a laser Doppler anemometer, confirmed the results of calculating the U component by equation (3). To obtain heat fluxes in the vicinity of a two-dimensional flame front from (2), the integration procedure was replaced by summation of finite differences.

3. Results and discussion

When burning in a laminar flow, the physical-chemical transformations are determined by the molecular transport processes that occur against the background of the general convective movement of gas. The study of relationship between heat fluxes of different natures is of particular interest: between the values of convective flux, reflecting energy transfer at directional displacement of a continuous medium, and molecular flow, which transfers heat through thermal conductivity inside a moving reacting gas. Within the framework of this task, the question about the influence of initial composition on the ratio between different transfer mechanisms arises, i.e., about data acquisition for the lean mixture and comparison with thermal parameters of the rich mixture.

To present the material, it is advisable to present expression (2) in a brief form. The terms of the left-hand side, reflecting the energy transfer through convection due to the directional movement of gas are denoted as *C*, and the terms of the right-hand side associated with energy dissipation due to heat conductivity are denoted as *M*. Thus, the energy equation has the form $C = M + W$, where

$$C = \left(\frac{\partial(\rho C_{\mathrm{P}} T \cdot V)}{\partial y} + \frac{1}{r} \cdot \frac{\partial(r \cdot \rho C_{\mathrm{P}} T \cdot U)}{\partial r} \right), \quad M = \frac{\partial}{\partial y}\left(\lambda \frac{\partial T}{\partial y} \right) + \frac{1}{r} \cdot \frac{\partial}{\partial r}\left(r \cdot \lambda \frac{\partial T}{\partial r} \right).$$

Below, there is a brief overview of data, which reveal the connection of the reacting flow parameters with the characteristic zones of the flame front: the position of maxima of the luminous region contour and heat release.

3.1. Heat release rate

In the present work and studies [22], the balance method in the energy equation was used to analyze the heat transfer processes. Based on the experimental data, the terms of equation (2) were determined, except the unknown, which was determined then from the condition that the left- and right-hand sides of this equation are equal, i.e., $W = C - M$ or

$$W = \left(\frac{\partial(\rho C_{\mathrm{P}} T \cdot V}{\partial y} + \frac{1}{r} \cdot \frac{\partial(r \cdot \rho C_{\mathrm{P}} T \cdot U}{\partial r} \right) - \left[\frac{\partial}{\partial y}\left(\lambda \frac{\partial T}{\partial y} \right) + \frac{1}{r} \cdot \frac{\partial}{\partial r}\left(r \cdot \lambda \frac{\partial T}{\partial r} \right) \right].$$

It can be seen from the above expression that it is not possible to obtain the value of heat release rate *W* without data on the gas velocity components, i.e., data about organization of a specific combustion process. The diagrams of changes in heat dissipation obtained in experiments with burning rich [22] and lean mixtures at $r = 2$ mm are presented in Fig. 7. The maximal heat release rate (500 ± 50 MW/m^3) in the lean mixture is higher here than in the rich mixture, apparently due to more complete combustion.

3.2. Energy transfer by heat conductivity and convection

The data obtained allow us to analyze the relation of mechanisms of convective and molecular heat transfer. The energy fluxes (MW/m^2) in the flame of rich and lean mixtures obtained by integrating the left- (*C*) and right- (*M*) hand sides of the energy equation containing thermal conductivity are compared in Fig. 8. Heat fluxes are the vector quantities, therefore, the minus sign is used for q_λ, as in the Fourier law. A negative value of projection of the molecular heat flux means that it is directed against the temperature gradient, i.e., towards the original mixture, and it is spent on its heating:

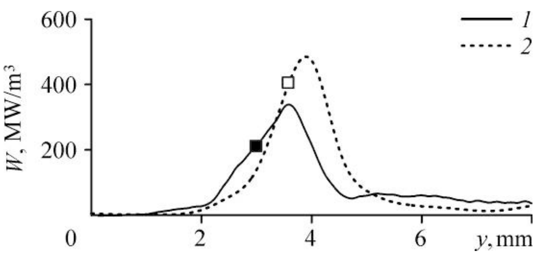

Fig. 7. A change in heat release with a distance from the wall for the rich and lean propane-butane-air mixtures. Symbols indicate the position of the visible flame contour; *1* — M-flame, *2* — V-flame.

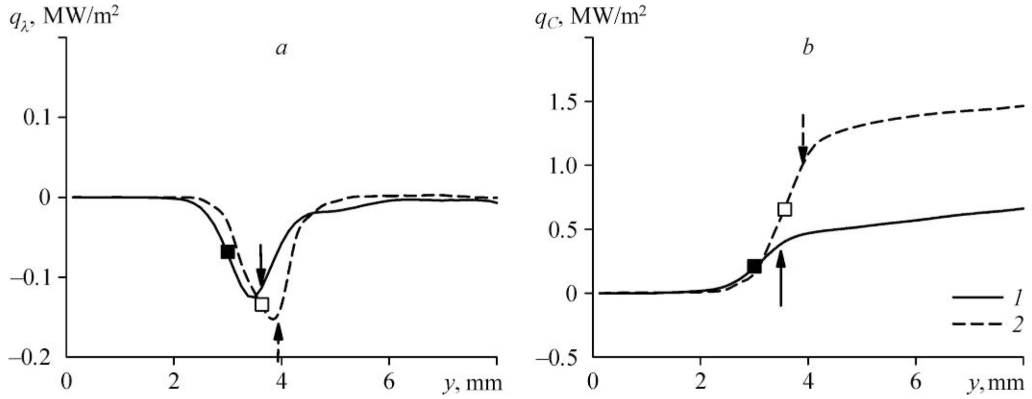

Fig. 8. Projections of energy fluxes caused by molecular (*a*) and convective transfer (*b*) on the jet axis for $r = 2$ mm at combustion of rich and lean propane-butane-air mixtures.
Symbols indicate the position of the visible flame contour, arrows — region of heat release; *1* — M-flame, *2* — V-flame.

$$\overrightarrow{q_C} = \int_0^y C \cdot dy \quad \overrightarrow{q_\lambda} = -\int_0^y M \cdot dy. \tag{4}$$

It can be seen in Fig. 8*a* that transfer by thermal conductivity becomes maximal in the vicinity of the flame front, whose position is indicated by arrows. Internal (molecular) heat transfer occurs against the background of convective motion caused by heating and thermal expansion of the reacting gas. When comparing the data in Figs. 8*a* and 8*b*, we can see that convective heat fluxes (Fig. 8*b*), which develop during physical-chemical transformations in a rich mixture, exceed significantly the internal molecular transfer through thermal conductivity. Thermal convection in the studied lean mixture (V-flame) is more intensive than in a rich mixture (M-flame).

The difference in heat fluxes of different nature (4) is determined by integral $\int_0^y W dy$, which is related to heat release in a chemically reacting gas flow, providing a balance in energy equation $C = M + W$. As a rule, the ratio of heat fluxes, similar to q_C / q_λ, is determined by Peclet and Stanton numbers. In the theory of combustion [21], to describe the diffusion burning, Peclet number of the gas flow $\mathrm{Pe} = \rho V r / (\lambda / C_\mathrm{P})$, characterizing the ratio of the convective and molecular transport mechanisms is used. In the theory of heat transfer [30], Stanton criterion $\mathrm{St} = q_\mathrm{w} / [\rho U_0 C_\mathrm{P} (T_0 - T_\mathrm{w})]$ is used for the ratio of heat fluxes on the wall and gas flow moving along it.

Conclusion

The aim of the study was to obtain experimental data on heat release and heat fluxes for the lean cellular flame and compare them with similar parameters of the rich mixture flame to study the effect of initial composition on thermal characteristics of the combustion process.

In experiments with axisymmetric flame, which is available for optical measurements, the CARS and PIV equipment was used. To analyze the empirical information, the balance method was used in the energy equation for Lewis–Semenov number Le = 1. We considered combustion of a lean ($\Phi = 0.9$) propane-butane-air mixture. Distribution of parameters was compared with the position of the characteristic regions in the vicinity of the combustion zone: maximal heat release and flame surface visualized by glow.

Convective and molecular heat transfers were estimated separately. At combustion of a lean propane-butane-air mixture, the molecular heat fluxes are higher than in the case of combustion of a rich mixture ($\Phi = 1.4$). In both cases, the heat fluxes caused by thermal conductivity reach their maxima at the center of the heat release zone. It is shown that in the case of rich mixture burning, molecular heat fluxes are significantly lower than convective ones, which, in turn, are almost twice as weak as convective flows in the flame of lean mixture. The maximal intensity of heat release in a rich mixture flame (~ 400 ± 50 MW/m^3) is lower than in a poor mixture (~ 500 ± 50 MW/m^3). It is also shown that in the case of combustion of a mixture of lean composition, the visible flame contour is an isothermal surface of 1100 ± 50 K. The rate of temperature rise from the initial to the final value exceeds significantly the rate of gas velocity increase, which may be a reason for a local increase in static pressure. It was revealed that in the absence of data on the velocity fields of the moving gas, it is impossible to determine the rate of heat release in experiments.

The performed analysis is qualitative rather than quantitative. Investigation results can be supplemented and refined with improvement of experimental equipment and methods for processing the measurement results.

Nomenclature

C_P — heat capacity, J/(kg·K),
d — diameter of furnace outlet, m,
λ — heat conductivity, W/(m·K),
ν — coefficient of kinematic viscosity of fuel and air mixture, m^2/s,
Pe = $\rho \cdot V \cdot r/(\lambda/C_P)$ — Peclet number,
Re = dV/ν — Reynolds number,
r — transverse coordinate, m,
ρ — density, kg/m^3,
St = $q_w \cdot \rho_0 \cdot U_0 \cdot C_P\,(T_w - T_0)$ — Stanton number,
T — temperature, K,
U — transverse component of velocity vector, m/s,
V — longitudinal component of velocity vector, m/s,
W — heat release rate, J/m^3,
y — longitudinal coordinate, m.

Subscripts

0 — parameters for the gas flow core, o — standard atmosphere, w — parameters on the wall.

References

1. **H.W. Coleman, R.J. Moffat, and W.M. Kayes,** Momentum and energy transport in the accelerated fully rough turbulent boundary layer, Thermosc. Div., Mech. Engng Dept., Stanford University, 1976, Report No. HMT-24.
2. **E.P. Volchkov, V.I. Terekhov, and V.V. Terekhov,** Flow structure and heat and mass transfer in boundary layers with injection of chemically reacting substances (review), Combustion, Explosion and Shock Waves, 2004, Vol. 40, No. 1, P. 3–20.
3. **E.P. Volchkov, N.A. Dvornikov, and L.N. Perepechko,** Comparison of different methods of modeling turbulent combustion in a boundary layer, Combustion, Explosion and Shock Waves, 1996, Vol. 32, No. 4, P. 390–394.
4. **L. Orloff, A.T. Modak, and R.L. Alpert,** Burning of large-scale vertical surfaces, 16th Symp. (Int.) on Combustion, Comb. Inst., 1976, Vol. 16, No. 1, P. 1345–1354.
5. **P.J. Paul, H.S. Mukunda, and V.K. Jain,** Regression rates in boundary layer combustion, 19th Symp. (Int.) on Combustion, Comb. Inst., 1982, Vol. 19, No. 1, P. 717–729.
6. **A.V. Singh and M.J. Gollner,** A methodology for estimation of local heat fluxes in steady laminar boundary layer diffusion flames, Combustion and Flame, 2015, Vol. 162, P. 2214–2230.
7. **E.P. Volchkov,** Near-Wall Gas Cooling, Nauka, Novosibirsk, 1983.
8. **V. Ali, V. Raghavan, and S. Tiwari,** A study of steady laminar diffusion flame over methanol pool surface, Int. J. Heat Mass Transfer, 2010, Vol. 53, P. 4696–4706.
9. **B.F. Boyarshinov, V.I. Titkov, and S.Yu. Fedorov,** Momentum transfer in the boundary layer when there is acceleration and combustion of ethanol as it evaporates behind a barrier, Combustion and Flame, 2010, Vol. 157, P. 1496–1509.
10. **B.F. Boyarshinov and S.Yu. Fedorov,** Heat and mass transfer and stabilization of combustion in the boundary layer behind a rib and a backward-facing step, Combustion, Explosion, and Shock Waves, 2013, Vol. 49, No. 5, P. 507–511.
11. **C.E.,Wooldridge and R.J. Muzzy,** Measurements in a turbulent boundary layer with porous wall injection and combustion, Tenth Symp. (Intern.) on Combustion, Pittsburg, The Combustion Institute, 1965, Vol. 10, No. 1, P. 1351–1362.
12. **E.P. Volchkov, V.I. Terekhov, and V.V. Terekhov,** Boundary-layer structure with hydrogen combustion with different injection intensities, Combustion, Explosion and Shock Waves, 2002, Vol. 38, No. 3, P. 269–277.

13. **V.V. Lukashov, V.V. Terekhov, and K. Hanjalić,** Heat exchange in boundary layer on permeable plate at injection and combustion, Thermophysics and Aeromechanics, 2013, Vol. 20, No. 6, P. 687–694.
14. **B.F. Boyarshinov,** Experimental investigation of the limits of ethanol combustion in the boundary layer behind an obstacle, Thermophysics and Aeromechanics, 2018, Vol. 25, No. 1, P. 47–54.
15. **R.Kh. Abdrakhmanov and B.F. Boyarshinov,** Experimental study of a cellular ethanol flame evaporating "on the ceiling", Combustion, Explosion and Shock Waves, 2018, Vol. 54, No. 1, P. 1–8.
16. **Turbulent reacting flows,** P.A. Libby, F.A. Williams (Eds.), Springer-Verlag, 1980.
17. **D. Bradly,** How fast can we burn?, in: 24th Symp. Int. on Comb., 1992, P. 247–262.
18. **C.J. Sung, J.B. Liu, and C.K. Law,** Structural response of counterflow diffusion flames to strain rate variations, Combustion and Flame, 1995, Vol. 102, P. 481–492.
19. **J.L. De Ris and L. Orloff,** Flame heat transfer between parallel panels, 8th Symp. (Int.) On Fire Safety Science, Proceedings, 2005, P. 999–1010.
20. **C.K. Law and C.J. Sung,** Structure, aerodynamics, and geometry of premixed flamelets, Progress in Energy and Combustion Sci., 2000, Vol. 26, P. 459–505.
21. **C.K. Law,** Combustion Physics, Cambridge University Press, 2006.
22. **R.Kh. Abdrakhmanov, B.F. Boyarshinov, and S.Yu. Fedorov,** Investigation of the local parameters of a cellular propane/butane/air flame, Int. J. Heat Mass Transfer, 2017, Vol. 109, P. 1172–1180.
23. **M. Stöhr, K. Oberleithner, C.M. Arndt, A.M. Steinberg, and W. Meier,** Experimental study of transient coupling of PVC formation and flame shape transition in a bi-stable turbulent swirl flame, in: Proc. European Combustion Meeting, 2015.
24. **O.V. Sharypov,** Introduction to Combustion Physics: Textbook, NSU, Novosibirsk, 2010.
25. **A.G. Istratov, N.I. Kidin, and A.V. Fedorov,** Cellular and tulip flame configurations, J. Appl. Mech. Tech. Phys., 2003, Vol. 44, No. 3, P. 395–399.
26. **X. Shena, X. Heb, and J. Sunc,** A comparative study on premixed hydrogen–air and propane–air flame propagations with tulip distortion in a closed duct, Fuel, 2015, Vol. 161, P. 248–253.
27. **Certificate No. 2017616085** on the Computer Program CARSspectra v.02. Priority of February 21, 2017. Author: S.Yu. Fedorov, Rightholder: IT SB RAS.
28. **A.N. Lipatnikov and J. Chomiak,** Effects of premixed flames on turbulence and turbulent scalar transport, Prog. Energy Combust. Sci., 2010, Vol. 36, P. 1–102.
29. **B.F. Boyarshinov,** Investigation of momentum and mass transfer in the turbulent boundary layer with ethanol combustion behind a barrier, S.M. Frolov (Ed.), Nonequilibrium Processes in Plasma, Combustion, and Atmosphere, Torus Press Ltd., Moscow, 2012, P. 221–227.
30. **S.I. Isaev, I.A. Kozhinov, V.I. Kofanov, A.I. Leontyev, B.M. Mironov, V.M. Nikitin, G.B. Petrazhitsky, M.S. Samoilov, V.I. Khvostov, and E.V. Shishov,** Theory of Heat and Mass Transfer, A.I. Leontiev (Ed.), Vysshaya Shkola, Moscow, 1979.